

Deficiency of retinoblastoma protein leads to inappropriate S-phase entry, activation of E2F-responsive genes, and apoptosis

(tumor suppressor gene/cell cycle control/programmed cell death)

ALEXANDRU ALMASAN*†‡, YUXIN YIN*†§, RUTH E. KELLY*, EVA Y.-H. P. LEE¶, ALLAN BRADLEY¶, WEIWEI LI**, JOSEPH R. BERTINO**, AND GEOFFREY M. WAHL*††

*Gene Expression Laboratory, The Salk Institute, 10010 North Torrey Pines Road, La Jolla, CA 92037; †Center for Molecular Medicine and Institute of Biotechnology, The University of Texas Health Science Center at San Antonio, San Antonio, TX 78284; ‡Department of Molecular and Human Genetics and Howard Hughes Medical Institute, Baylor College of Medicine, Houston, TX 77030; and **Program for Molecular Pharmacology and Therapeutics, Memorial Sloan-Kettering Cancer Center, New York, NY 10021

Communicated by Leslie E. Orgel, The Salk Institute for Biological Studies, San Diego, CA, January 24, 1995 (received for review December 12, 1994)

ABSTRACT The retinoblastoma susceptibility gene (*Rb*) participates in controlling the G₁/S-phase transition, presumably by binding and inactivating E2F transcription activator family members. Mouse embryonic fibroblasts (MEFs) with no, one, or two inactivated *Rb* genes were used to determine the specific contributions of Rb protein to cell cycle progression and gene expression. MEFs lacking both *Rb* alleles (*Rb*^{-/-}) entered S phase in the presence of the dihydrofolate reductase inhibitor methotrexate. Two E2F target genes, dihydrofolate reductase and thymidylate synthase, displayed elevated mRNA and protein levels in *Rb*⁻ MEFs. Since absence of functional Rb protein in MEFs is sufficient for S-phase entry under growth-limiting conditions, these data indicate that the E2F complexes containing Rb protein, and not the Rb-related proteins p107 and p130, may be rate limiting for the G₁/S transition. Antineoplastic drugs caused accumulation of p53 in the nuclei of both *Rb*^{+/+} and *Rb*^{-/-} MEFs. While p53 induction led to apoptosis in *Rb*^{-/-} MEFs, *Rb*^{+/+} and *Rb*^{+/-} MEFs underwent cell cycle arrest without apoptosis. These results reveal that diverse growth signals work through *Rb* to regulate entry into S phase, and they indicate that absence of Rb protein produces a constitutive DNA replication signal capable of activating a p53-associated apoptotic response.

The retinoblastoma tumor suppressor gene (*Rb*) encodes a nuclear phosphoprotein that participates in the transition between G₁ and S phases of the cell cycle (1). The Rb protein is phosphorylated in several stages during the cell cycle, starting at a point after mid-G₁ (2–6), most likely by cyclin D-cdk4, cyclin D-cdk6 (7), or perhaps cyclin E-cdk2 complexes (8, 9). Hypophosphorylated Rb protein is required for growth suppression, as microinjection of Rb can prevent S-phase entry (2).

The viral oncoproteins adenovirus E1A, simian virus 40 T antigen, and oncogenic human papilloma virus (HPV) E7 bind hypophosphorylated Rb protein (see refs. 1 and 10 for reviews and references). Oncoprotein binding and hyperphosphorylation have been proposed to displace cellular Rb-binding proteins such as the E2F family of transcriptional activators. The capacity of Rb protein to cause cell cycle arrest is dependent on sequences important for its interaction with E2F (1, 10). Overexpression of the cDNA for E2F-1 reverses Rb protein-mediated G₁ arrest and promotes S-phase entry (11), presumably through transactivation of E2F-1 target genes such as those encoding dihydrofolate reductase (DHFR) (12, 13) and

thymidylate synthase (TS) and other genes necessary for entry into and progression through S phase (10, 14).

The data obtained from studies with viral oncoproteins suggest that Rb protein acts by sequestering essential factors required for G₁/S progression. However, each of these oncoproteins binds other cellular factors such as the Rb-related proteins p107, p130, p300, and multimeric kinase complexes containing p107 and cyclin A/cdk2 or cyclin E/cdk2 (1, 10). Thus, some of the effects imputed to derive from Rb protein binding may actually relate to inactivation of other cellular proteins involved in the G₁/S transition. Furthermore, the potential effects of releasing E2F from Rb protein have been based primarily on transient transfection experiments with reporter constructs. Such experiments do not address the specific metabolic and cell cycle consequences of relieving E2F family members from inhibitory binding solely to the Rb protein.

This study addresses the specific impact of Rb protein deficiency on S-phase entry and progression by using a defined genetic system in which an *Rb* mutation is the sole genetic change. One or both *Rb-1* alleles were previously inactivated by using homologous recombination in mouse embryonic stem (ES) cells to destroy the regions in the Rb protein that bind E2F-1 (15–17). We show that fibroblasts derived from mouse embryos (MEFs) lacking functional Rb protein resulted in elevated mRNA and protein levels of E2F target genes. Furthermore, all MEFs, regardless of Rb protein status, accumulated p53 in their nuclei as a result of treatment with a broad spectrum of antineoplastic drugs. However, p53 induction led to apoptosis in *Rb*^{-/-} MEFs but growth arrest in *Rb*^{+/+} or *Rb*^{+/-} MEFs. These results indicate that a balance of the levels of targets regulated by both p53 and Rb proteins controls successful entry into S phase and that misregulation of Rb protein targets triggers apoptosis when diverse growth challenges elevate p53 levels.

MATERIALS AND METHODS

Cell Culture and Nucleic Acid Analysis. MEFs containing wild-type or disrupted *Rb-1* genes were obtained from em-

Abbreviations: HPV, human papilloma virus; Mtx, methotrexate; F-Mtx, fluoresceinated MTX; DHFR, dihydrofolate reductase; TS, thymidylate synthase; MEF, primary mouse embryo fibroblast; FBS, fetal bovine serum; VP16, etoposide; Cam, camptothecin; araC, cytosine arabinonucleoside; PALA, *N*-(phosphonoacetyl)-L-aspartate. †A.A. and Y.Y. contributed equally to this work.

‡Present address: Departments of Cancer Biology and Radiation Oncology, Cleveland Clinic Foundation, Cleveland, OH 44195.

§Present address: Curriculum in Genetics and Molecular Biology, School of Medicine, University of North Carolina at Chapel Hill, Chapel Hill, NC 27599.

††To whom reprint requests should be addressed.

The publication costs of this article were defrayed in part by page charge payment. This article must therefore be hereby marked "advertisement" in accordance with 18 U.S.C. §1734 solely to indicate this fact.

bryos derived by the mating of heterozygous animals generated by homologous recombination at the *Rb-1* locus in ES cells (15). MEF genotype was determined by using the restriction digestion and DNA blotting strategies described previously (data not shown; see ref. 15). *Rb*^{+/+}, *Rb*^{+/-}, *Rb*^{-/-}, and *p53*^{-/-} MEFs, generated from 13-day-old knock-out mouse embryos (15, 18), were grown in Dulbecco's modified Eagle's medium (DMEM) containing 10% fetal bovine serum (FBS) (HyClone). Drug treatments were carried out in 10% dialyzed FBS. Serum withdrawal experiments used 0.5% FBS. All experiments were performed before the cultures reached passage 10. Methotrexate (Mtx), etoposide (VP16), camptothecin (Cam), and cytosine arabinonucleoside (araC) were obtained from Sigma; *N*-(phosphonoacetyl)-L-aspartate (PALA) was from the National Cancer Institute.

Total RNA was extracted by using RNAzol (Tel-Test, Friendswood, TX), separated by electrophoresis on an agarose/glyoxal gel, transferred to a nylon membrane, and then treated to reverse glyoxylation. Hybridization was performed as described previously, using random primed cDNA probes for the TS (19), DHFR (20), and human acidic ribosomal phosphoprotein 36B4 mRNAs (21).

Flow Cytometry. DHFR enzyme levels were determined in individual cells by using an assay based on binding of fluoresceinated-Mtx (F-Mtx) to the DHFR protein and microfluorimetry (22, 23). Cells (2×10^6) were treated for 24 hr with 3 μ M F-Mtx. A second cell population was treated with Mtx in addition to F-Mtx to reveal background fluorescence due to nonspecific binding of F-Mtx. Hypoxanthine and thymidine were added to all cultures to overcome potential inhibitory effects of F-Mtx. The cell cycle effects of Mtx were determined by treating exponentially growing MEF cultures with 200 nM Mtx for 48 hr, followed by flow cytometric analysis using previously published procedures (24–26).

Immunofluorescence. Cells grown on glass coverslips were washed with PBS (137 mM NaCl/2.7 mM KCl/4.3 mM Na₂HPO₄/1.4 mM KH₂PO₄, pH 7.3)/0.05% Tween 20 (PT), sequentially fixed at -20°C for 5 min in acetone followed by methanol, and washed again in PT. After a 2-hr incubation with the anti-p53 monoclonal antibody pAb421 (1:30 in PT, Oncogene Science), coverslips were washed with PT, incubated for 60 min with a biotinylated goat fluorescein isothiocyanate (FITC)-conjugated anti-mouse IgG antibody (1 μ g/ml; Oncogene Science), rinsed in PT, and mounted in Gelvatol (15% polyvinylalcohol/35% glycerol in PBS, pH 7.3). Cells were viewed with a Zeiss epifluorescence microscope and photographed with Ektachrome (Kodak) 400 ASA color slide film.

Analysis of Apoptosis in Rb Protein-Deficient Cells. Cells were treated for 24–48 hr with 50–1000 nM Mtx, 50 μ M or 1 mM PALA, 1 mM araC or Cam, and 5 mM VP16. Low molecular weight DNA was purified from pools of adherent and nonadherent cells according to a published procedure (27), separated on 1.3% agarose gels, and visualized by ethidium bromide staining.

RESULTS

Mtx Prevents *Rb*^{+/+} and *Rb*^{+/-}, but not *Rb*^{-/-}, MEFs from Progressing Through S Phase. We analyzed the consequences of *Rb-1* gene inactivation in primary fibroblasts derived from *Rb*-deficient knock-out mouse embryos (15) to investigate the specific role of Rb protein on cell cycle control in cells with otherwise normal genomes. Since Rb protein binding to E2F-1 has been proposed to regulate the expression of genes containing E2F response elements, we first determined whether *Rb-1* expression has an impact on cell cycle arrest induced by Mtx, a commonly used chemotherapeutic agent that inhibits the E2F target gene DHFR.

The experiment was performed in a blinded fashion: the cell cycle responses of embryonic fibroblasts from 14 embryos derived from an *Rb*^{+/+} \times *Rb*^{+/+} mating were scored prior to determining their genotype by Southern blotting (data not shown). The cell cycle profiles of fibroblasts containing or lacking functional *Rb* genes were indistinguishable in the absence of Mtx. However, Mtx arrested the majority of cells in 12 of 14 populations in late G₁ or early S phase (Fig. 1 *B* and *C*). The arrest was prevented when thymidine was added with Mtx (data not shown), indicating that thymidylate pools were rate limiting under the conditions employed. Southern blotting showed that each of these MEF strains contained at least one wild-type *Rb* allele (data not shown). In contrast, a significant fraction of cells in each of two MEF populations (Fig. 1*D*) entered and traversed much of S phase in the presence of Mtx. DNA blotting analysis revealed that these MEFs contain only the 6.5-kb *Hind*III fragment expected to be generated by insertion of the targeting vector into exon 20 of the *Rb-1* gene (data not shown; see ref. 15 for details). Sequential immunoprecipitation with monoclonal antibodies recognizing p53 in wild-type or mutant conformation showed the presence of only wild-type p53 in these *Rb*^{-/-} MEFs, indicating that the abnormal cell cycle response is not due to acquisition of p53 mutations during the *in vitro* growth of *Rb*^{-/-} MEFs (data not shown). These data support a close correlation between loss of Rb function and the G₁/S arrest caused by Mtx.

Activation of E2F Target Genes. Mtx interferes with thymidylate synthesis. Loss of functional Rb protein and the consequent transcription of E2F target genes such as TS and DHFR might, therefore, elevate thymidylate pools sufficiently to enable MEFs to cycle when challenged with Mtx. We measured the TS and DHFR mRNA levels in MEFs to test this hypothesis. Fig. 2*A* shows that TS and DHFR mRNA levels are 3- to 4-fold higher in *Rb*^{-/-} MEFs (lanes 4 and 5) than in *Rb*^{+/+} (lanes 1, 3, and 6) or *Rb*^{+/-} (lanes 2 and 7) MEFs.

We next determined whether elevated DHFR protein was produced in the *Rb*^{-/-} MEFs by using a flow microfluorimetry assay that measures the intracellular binding of DHFR to F-Mtx (22, 23). Fig. 2 *B* and *C* shows that *Rb*^{-/-} MEFs have a mean 2- to 3-fold increase in DHFR protein per cell, compared with *Rb*^{+/+} or *Rb*^{+/-} MEFs. However, this difference in DHFR protein levels is a mean value obtained from 10,000 cells. Importantly, the flow histogram of the *Rb*^{-/-} cells is broader than that of the *Rb*^{+/+} cells, indicating a substantial heterogeneity in DHFR protein levels in individual cells of the population. *Rb*^{-/-} cells at the extreme end of the distribution contain at least 10 times more DHFR protein than *Rb*^{-/-} cells at the center of the distribution (Fig. 2*B*). The elevated DHFR

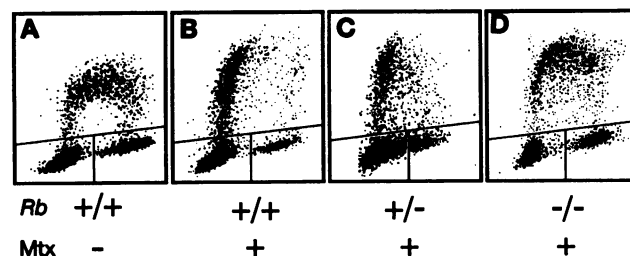


FIG. 1. Abrogation of G₁/S-arrest response to Mtx in *Rb*^{-/-} MEFs. MEFs containing two (strain Rb-1, *A* and *B*), one (strain Rb-4, *C*), or no (strain Rb-12, *D*) functional *Rb-1* alleles were treated with 200 nM Mtx for 48 hr. Mtx challenge of 12 MEF strains (e.g., Rb-1 and -4) produced a late G₁ or early S-phase arrest, while two strains (Rb-9 and -12) entered S phase. The DNA content, measured by propidium iodide staining of cells, is represented as a linear scale on the abscissa, showing cells with 2*N* or 4*N*, respectively, in G₁ (lower left of each panel) and G₂/M (lower right of each panel). The ordinate is a logarithmic scale representing cells in S phase, based on incorporation of 5-bromodeoxyuridine.

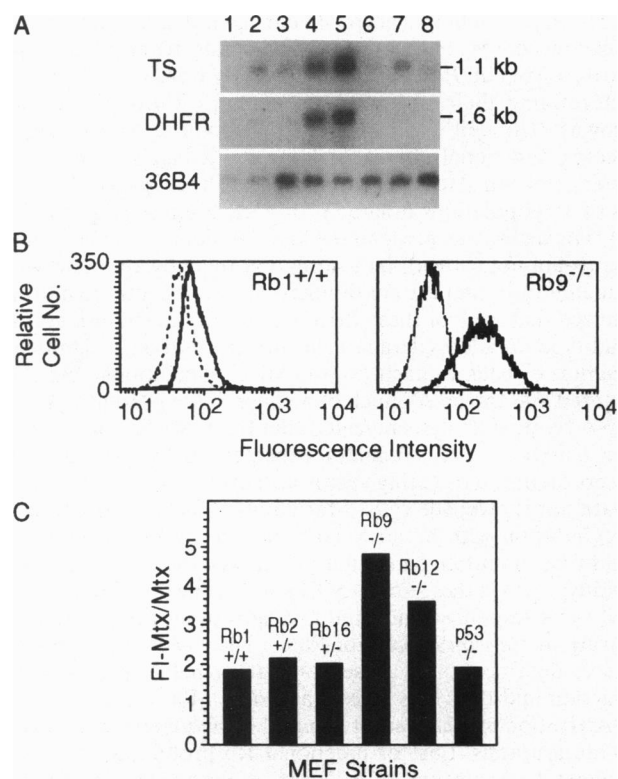


FIG. 2. Increased synthesis of DHFR and TS in Rb protein-deficient cells. (A) mRNA levels. RNA blot hybridization was conducted sequentially with the mouse TS, DHFR, and 36B4 cDNAs, the latter being used as an internal control for the amount of RNA loaded, transferred, and hybridized. The following MEF strains were analyzed in lanes 1–8, respectively: 1, $Rb^{+/+}$; 2, $Rb^{+/+}$; 6, $Rb^{+/+}$; 9, $Rb^{-/-}$; 12, $Rb^{-/-}$; 13, $Rb^{+/+}$; 14, $Rb^{+/+}$; and 16, $Rb^{+/+}$. Hybridization signal quantification, using a PhosphorImager (Molecular Dynamics), revealed an approximately 3-fold increase in TS and DHFR mRNA levels in $Rb^{-/-}$ (lanes 4 and 5) as compared with $Rb^{+/+}$ or $Rb^{+/+}$ MEFs after correction for the internal standard. (B) DHFR protein levels in individual cells. Protein levels in logarithmically growing $Rb^{+/+}$ and $Rb^{-/-}$ cells were determined by F-Mtx binding and flow microfluorimetry (22, 23). For each strain, the right peak represents F-Mtx binding to DHFR and the left peak provides a measure of background fluorescence of cells treated with MTx in addition to F-Mtx. (C) Mean DHFR protein levels determined by F-Mtx (FI-Mtx) binding. The DHFR levels in individual cells were calculated by determining the ratio of the means of the flow microfluorimetry values of cells treated with F-Mtx or F-Mtx + MTx. There is a good correlation between the relative increases in DHFR mRNA and the mean F-Mtx binding capacity in populations of $Rb^{-/-}$ relative to $Rb^{+/+}$ and $Rb^{+/+}$ MEFs. $Rb^{+/+}$ MEF populations had marginally higher F-Mtx binding levels than $Rb^{+/+}$ cells. Note that the growth rate of MEFs does not have a significant impact on the DHFR protein levels, as $p53^{-/-}$ $Rb^{+/+}$ MEFs exhibited approximately the same DHFR content as $p53^{+/+}$ $Rb^{+/+}$ MEFs.

expression in $Rb^{-/-}$ cells is not an indirect result of the presence of more S-phase cells in the faster-growing $Rb^{-/-}$ population, since rapidly growing $p53^{-/-}$ $Rb^{+/+}$ MEFs express nearly the same amount of DHFR protein as wild-type MEFs (Fig. 2C).

Nuclear Accumulation of p53. Previous work with viral and transfection systems indicated that p53 and Rb protein work in concert to regulate entry into S phase after DNA damage (28, 29). We therefore investigated whether the constitutive expression of S-phase-associated genes in $Rb^{-/-}$ cells might have an impact on the levels or cellular localization of p53 under a variety of growth conditions.

The intracellular localization of the p53 protein was examined by immunofluorescent staining (Fig. 3). The p53 staining

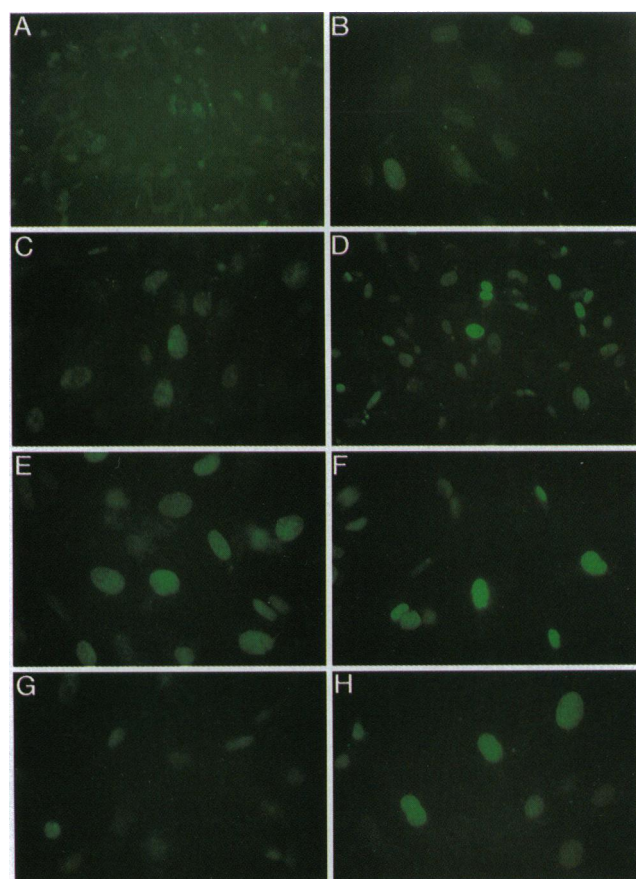


FIG. 3. p53 cellular localization following growth challenge. p53 levels in $Rb^{+/+}$ (A, C, E, and G) and $Rb^{-/-}$ (B, D, F, and H) MEFs were analyzed by immunofluorescence using the p53-specific antibody pAb421. Untreated MEFs (A and B) revealed low, homogenous levels of predominantly nuclear p53. MTx (C and D) or Cam (E and F) treatment elevated nuclear p53 staining in both $Rb^{+/+}$ and $Rb^{-/-}$ cells to approximately the same extent. By contrast, p53 levels were higher in the nuclei of $Rb^{-/-}$ (H) compared with $Rb^{+/+}$ (G) cells grown in 0.5% serum.

in untreated $Rb^{+/+}$ (A) and $Rb^{-/-}$ (B) MEFs was diffuse and relatively weak, with most of the p53 localized to the cytoplasm. While most cells in the population expressed similar levels of p53, this protein was localized to nuclei in a small percentage of $Rb^{-/-}$ cells. The anti-p53 fluorescence in $Rb^{+/+}$ and $Rb^{-/-}$ MEFs treated with MTx (D) or Cam (F) was predominantly nuclear and far more intense than in untreated cells. However, considerable heterogeneity in p53 levels was noted from cell to cell in both populations. By contrast, serum deprivation significantly elevated nuclear p53 levels only in $Rb^{-/-}$ MEFs [compare Fig. 3H ($Rb^{-/-}$) with G ($Rb^{+/+}$)]. These experiments have been repeated at least six times for each treatment, with similar results. The results indicate that similar fractions of the $Rb^{-/-}$ and $Rb^{+/+}$ cell populations accumulate apparently equivalent amounts of nuclear p53 in response to antimitabolites or topoisomerase inhibitors, while the two genotypes respond differently to serum deprivation. The heterogeneity of p53 levels suggests that only a subset of cells process the signals generated by these growth challenges, perhaps because they are in a particular phase of the cell cycle.

Apoptosis in Cells Treated with Antineoplastic Drugs or Grown Under Nutrient-Limiting Conditions. We occasionally observed p53 accumulation in small structures in $Rb^{-/-}$ but not in $Rb^{+/+}$ MEFs (data not shown). These structures resemble the apoptotic bodies observed after γ -irradiation of mouse hepatoma cells (30). In addition, a significant proportion of MTx-treated $Rb^{-/-}$, but not $Rb^{+/+}$, MEFs detached

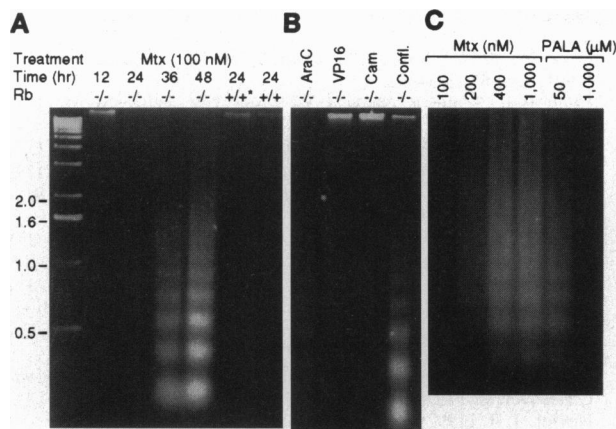


FIG. 4. Apoptosis in *Rb* protein-deficient MEFs. (A) Mtx-induced apoptosis depends on *Rb* genotype. DNA isolated from Mtx-treated exponentially growing *Rb*^{-/-} cells displayed a DNA ladder 24–48 hr after drug addition. This was not detected in similarly treated *Rb*^{+/+} *p53*^{-/-} (designated *Rb* +/+*) or *Rb*^{+/+} MEFs. (B) Effects of araC, VP16, Cam, and growth factor removal on apoptosis. Treatment (36 hr) of *Rb*^{-/-} cells with the indicated drugs generated a DNA ladder. Cells kept confluent for 48 hr generated a DNA ladder of an intensity similar to that observed in cells passaged in low serum. (C) Differential effects of Mtx and PALA in *Rb*^{-/-} cells. Mtx treatment (24 hr) generated a dose-dependent apoptotic response from 100 to 1000 nM. In contrast, apoptosis was observed in cells treated with 50 μM but not 1 mM PALA. The DNA was resolved on 1.3% agarose gels and visualized by ethidium bromide staining. Numbers on left indicate the positions of size standards (in kb).

from the culture plates beginning 36 hr after Mtx treatment. These observations led us to investigate whether growth challenges specifically activate the apoptotic death pathway in *Rb*^{-/-} cells. Fig. 4 shows that DNA prepared from Mtx-treated *Rb*^{-/-} cells contained the 180- to 200-bp DNA ladder generated by internucleosomal cleavage, which is the hallmark of apoptotic cell death (31). The characteristic DNA ladder in *Rb*^{-/-} MEFs appeared 24 hr after Mtx treatment (Fig. 4A). However, this pattern was not observed in similarly treated *Rb*^{+/+} *p53*^{-/-} or *Rb*^{+/+} MEFs. Therefore, loss of both *Rb* alleles is required to trigger Mtx-induced apoptosis. Interestingly, higher Mtx concentrations resulted in a higher intensity of the DNA ladder, indicating recruitment of additional cells into the apoptotic pathway (Fig. 4C).

Apoptosis was also induced after treatment with antineoplastic agents such as VP16, araC, or Cam (Fig. 4B), which are known to induce DNA damage and have been previously shown to induce apoptosis in other cell types. In contrast, treatment with the antimetabolite PALA induced apoptosis only at lower concentrations (50 μM). As the PALA concentration was increased from 50 to 1000 μM, the DNA ladder disappeared (Fig. 4C), corresponding to the capacity of the respective drug dose to induce G₁ arrest (data not shown). Apoptotic death was not limited to *Rb*^{-/-} cells challenged with DNA-damaging agents. Confluence (Fig. 4B) or serum deprivation (data not shown) also induced DNA fragmentation. These results clearly implicate *Rb* protein in a cell death pathway in response to diverse natural and drug-induced growth challenges.

DISCUSSION

This study employed MEFs containing inactivated alleles of the *Rb-1* tumor suppressor gene to assess the specific impact of *Rb* protein function on gene expression and cell cycle control. The data demonstrate that functional *Rb* is essential for regulating the conditions under which cells enter S phase and the consequences of entry under growth-limiting condi-

tions. As one example, MEFs containing at least one functional *Rb* gene became arrested near the G₁/S boundary when challenged with Mtx, while MEFs devoid of functional *Rb* entered S phase under identical conditions. *Rb*^{-/-} MEFs expressed elevated levels of mRNAs encoded by DHFR and TS genes, two genes which are regulated by E2F, a transcriptional activator sequestered by hypophosphorylated *Rb* protein. The significant increase in DHFR protein in *Rb*^{-/-} MEFs enables them to enter S phase in the presence of Mtx, which probably results in DNA damage. Importantly, the errant proliferation of *Rb*^{-/-} MEFs under a variety of growth challenges correlated with accumulation of nuclear p53 and eventual death of treated populations by apoptosis. Similar treatment of *Rb*^{+/+} or *Rb*^{+/-} MEFs also increased p53 but did not induce apoptosis. These data imply that coordinating the regulation of genes or the activities of proteins affected by these tumor suppressors determines whether cells live or die in response to diverse growth challenges.

Our studies show that the interaction between *Rb* protein and specific E2F family members may cause many E2F target genes to be rate limiting for progression into S phase. Studies showing that microinjection of E2F allows cells to enter S phase (11) and that E2F overexpression increases expression of synthetic substrates harboring E2F binding sites (11, 13) are consistent with this interpretation. Furthermore, inactivation of *Rb* by intragenic mutation (ref. 26 and unpublished results) or by extragenic modifiers that produce *Rb* protein hyperphosphorylation (unpublished results) also generated a 2- to 4-fold increase in DHFR mRNA and protein levels. As the latter results were obtained in human cancer cell lines derived from multiple organ systems, *Rb* protein may be rate limiting for the expression of E2F target genes in diverse cell lineages.

Recent *in vitro* binding studies indicate that the *Rb* protein is a minor contributor to E2F binding and suggest that p130 and p107 are major regulators of a subset of E2F functions in late G₀ or early G₁ and in late G₁, respectively (32). It is surprising, therefore, that loss of *Rb* function occurs in many human cancers (1) and causes early embryonic lethality in mice (15–17), while inactivating mutations in the p107 gene have not been detected in human tumors (M. Ewen, personal communication), and no phenotype has been observed in p107-deficient mice (T. Jacks, personal communication). The profound alterations in gene expression and cell cycle control that we can now specifically attribute to the interaction between *Rb* and some E2F family members provide a molecular explanation for the frequent targeting of this tumor suppressor gene by diverse oncoproteins and inactivating mutations in human tumors. However, it is possible that *Rb*-related proteins may play important roles in the G₁/S transition of other cell types, or under conditions different from those studied here, or that they might regulate cell cycle exit during differentiation of specific lineages. Furthermore, as many proteins in addition to E2F bind *Rb* protein (1, 10), it is possible that the phenotypic effects observed in *Rb*^{-/-} MEFs derive from the cumulative effects of misregulation of multiple *Rb* protein targets.

Rb protein function is required for the p53-mediated arrest induced by γ-irradiation and other growth challenges (26, 33). The γ-irradiation-induced arrest does not take place in cell lines expressing HPV E7 (26, 28, 29) and in *Rb*^{-/-} MEFs (26, 29). This implies that constitutive expression of genes that are otherwise blocked as a consequence of *Rb* protein binding to E2F, and perhaps other regulatory proteins, underlies the ability of *Rb*^{-/-} cells to enter S phase inappropriately. Thus, although all p53 target genes should be functional in the *Rb*^{-/-} MEFs, the deficiency of *Rb* in these cells precludes activation of some, but not all, p53-mediated arrest mechanisms (see below).

The consequences of p53 activation on cell cycle progression and cell viability differ dramatically depending on the *Rb* genotype. Absence of *Rb* function apparently allows sufficient

synthesis of gene products required for S-phase entry to allow cell cycle progression under conditions that arrest $Rb^{+/+}$ MEFs. While similar nuclear p53 accumulation was elicited by such conditions in both $Rb^{-/-}$ and $Rb^{+/+}$ cells, only cells lacking functional Rb protein underwent apoptosis. These observations are consistent with another study in which overexpression of E2F in the presence of wild-type p53 induced apoptosis (34). Ubiquitous Rb deficiency in knock-out mice (15–17) or selective Rb protein inactivation by targeted expression of HPV E7 or of a mutated simian virus 40 T antigen which cannot bind p53 (35–38) resulted in ectopic mitoses and apoptosis *in vivo*. By contrast, inactivation of p53 in cells lacking functional Rb protein led to hyperproliferation and increased frequency of tumorigenesis (35, 36). Thus, it is likely that the apoptosis induced by various conditions in the $Rb^{-/-}$ MEFs can be attributed to the increased abundance of nuclear p53 we observed in $Rb^{-/-}$ cells. The p53–Rb check and balance system provides an effective means of limiting the emergence of genetic variants containing amplified, deleted, or translocated chromosomal regions, which can be formed by chromosome breakage induced by S-phase progression under limiting metabolic conditions (24, 26). Nevertheless, apoptosis is not limited to Rb-deficient cells, since overexpression of c-myc (39) or E1A (40), which also promote unscheduled proliferation, also leads to apoptosis following certain growth challenges.

Early embryonic death in $Rb^{-/-}$ mice was attributed in part to an inability of certain cell lineages to differentiate (15–17). Our data on apoptosis induced by growth factor deprivation in $Rb^{-/-}$ MEFs suggest an alternative interpretation. We propose that Rb protein deficiency generates a constitutive signal to proceed from G₁ into S phase. Exposure of $Rb^{-/-}$ cells to terminal differentiation cues may then generate a conflicting negative signal that can be transduced through p53 or other regulatory systems and result in apoptosis in some, although not necessarily all, cell lineages (41). The ectopic mitoses and apoptosis observed in neuronal tissues of $Rb^{-/-}$ embryos (15–17, 38) are consistent with this proposal. Thus, the prevalence of immature cells in some cell lineages in $Rb^{-/-}$ mice may reflect not their inability to differentiate but rather the active elimination of cells that attempt to obey differentiation signals.

An unexpected finding was that two antiproliferative agents that interfere with nucleotide synthesis exhibited different effects on cell viability depending on p53 or Rb genotype. Thus, increasing Mtx concentration resulted in more $Rb^{-/-}$ cells undergoing apoptosis, while increasing PALA concentration produced cell cycle arrest. By contrast, treatment of p53^{-/-} cells with increasing PALA concentration resulted in more cells dying, although it is unclear whether they were undergoing apoptosis (24). This provides an example of how determining p53 or Rb functional status could enable prediction of the efficiency of cell killing in response to dose escalation of drugs that appear to have similar mechanisms of action. Knowledge of the functional integrity of G₁/S control in cancer cells could provide a conceptual basis for improved chemotherapeutic strategies.

We thank V. Doucas and J. Trotter for assistance with immunofluorescence and flow cytometry, S. Rivera and M. Wims for molecular analyses of mouse fibroblasts, and L. F. Johnson (Ohio State University) for the PMTS (TS) cDNA probe. This work was supported by grants from the National Cancer Institute and the National Institute of General Medical Sciences to G.M.W., from the National Institute of Child Health and Human Development to A.B., from the National Cancer Institute to J.R.B., and from the National Cancer Institute and the National Institute of Child Health and Human Development (HD 30265) to E.Y.-H.P.L.; A.B. is an Associate Investigator with the Howard Hughes Medical Institute.

- Wang, J. Y. J., Knudsen, E. S. & Welch, P. J. (1994) *Adv. Cancer Res.* **64**, 25–85.
- Goodrich, D. W., Wang, N. P., Qian, Y. W., Lee, E. Y. & Lee, W. H. (1991) *Cell* **67**, 293–302.
- Chen, P. L., Scully, P., Shew, J. Y., Wang, J. Y. & Lee, W. H. (1989) *Cell* **58**, 1193–1198.
- DeCaprio, J. A., Furukawa, Y., Ajchenbaum, F., Griffin, J. D. & Livingston, D. M. (1992) *Proc. Natl. Acad. Sci. USA* **89**, 1795–1798.
- Lees, J. A., Buchkovich, K. J., Marshak, D. R., Anderson, C. W. & Harlow, E. (1991) *EMBO J.* **10**, 4279–4290.
- Lin, B. T., Gruenewald, S., Morla, A. O., Lee, W. H. & Wang, J. Y. (1991) *EMBO J.* **10**, 857–864.
- Ewen, M. E., Sluss, H. K., Sherr, C. J., Matsushime, H., Kato, J. & Livingston, D. M. (1993) *Cell* **73**, 487–497.
- Hinds, P. W., Mittnacht, S., Dulic, V., Arnold, A., Reed, S. I. & Weinberg, R. A. (1992) *Cell* **70**, 993–1006.
- Hatakeyama, M., Brill, J. A., Fink, J. R. & Weinberg, R. A. (1994) *Genes Dev.* **8**, 1759–1771.
- Nevins, J. R. (1992) *Science* **258**, 424–429.
- Johnson, D. G., Schwarz, J. K., Cress, W. D. & Nevins, J. R. (1993) *Nature (London)* **365**, 349–352.
- Blake, M. C. & Azizkhan, J. C. (1989) *Mol. Cell. Biol.* **9**, 4994–5002.
- Slansky, J. E., Li, Y., Kaelin, W. G. & Farnham, P. J. (1993) *Mol. Cell. Biol.* **13**, 1610–1618.
- Farnham, P. J., Slansky, J. E. & Kollmar, R. (1993) *Biochim. Biophys. Acta* **1155**, 125–131.
- Lee, E. Y., Chang, C.-Y., Hu, N., Wang, Y.-C., Lai, C.-C., Herrup, K., Lee, W.-H. & Bradley, A. (1992) *Nature (London)* **359**, 288–294.
- Jacks, T., Fazeli, A., Schmitt, E. M., Bronson, R. T., Goodell, M. A. & Weinberg, R. A. (1992) *Nature (London)* **359**, 295–300.
- Clarke, A. R., Maandag, E. R., van Roon, M., van der Lugt, N. M., van der Valk, M., Hooper, M. L., Berns, A. & te Riele, H. (1992) *Nature (London)* **359**, 328–330.
- Donehower, L. A., Harvey, M., Slagle, B. L., McArthur, M. J., Montgomery, C. A., Butel, J. S. & Bradley, A. (1992) *Nature (London)* **356**, 215–221.
- Deng, T. L., Li, D. W., Jenh, C. H. & Johnson, L. F. (1986) *J. Biol. Chem.* **261**, 16000–16005.
- Mclvor, R. S. & Simonsen, C. C. (1992) *Nucleic Acids Res.* **18**, 7025–7032.
- Laborda, J. (1991) *Nucleic Acids Res.* **19**, 3998.
- Gaudray, P., Trotter, J. & Wahl, G. M. (1986) *J. Biol. Chem.* **261**, 6285–6292.
- Kaufman, R. J., Bertino, J. R. & Schimke, R. T. (1978) *J. Biol. Chem.* **253**, 5852–5860.
- Yin, Y., Tainsky, M. A., Bischoff, F. Z., Strong, L. C. & Wahl, G. M. (1992) *Cell* **70**, 937–948.
- Di Leonardo, A., Linke, S., Clarkin, K. & Wahl, G. M. (1994) *Genes Dev.* **8**, 2540–2551.
- Almasan, A., Linke, S., Paulson, T., Huang, L.-c. & Wahl, G. M. (1995) *Cancer Metastasis Rev.* **14**, 59–73.
- Walker, P. R., Kokileva, L., LeBlanc, J. & Sikorska, M. (1993) *BioTechniques* **15**, 1032–1040.
- Demers, G. W., Foster, S. A., Halbert, C. L. & Galloway, D. A. (1994) *Proc. Natl. Acad. Sci. USA* **91**, 4382–4386.
- Slebos, R. J., Lee, M. H., Plunkett, B. S., Kessis, T. D., Williams, B. O., Jacks, T., Hedrick, L., Kastan, M. B. & Cho, K. R. (1994) *Proc. Natl. Acad. Sci. USA* **91**, 5320–5324.
- Unger, C., Kress, S., Buchmann, A. & Schwarz, M. (1994) *Cancer Res.* **54**, 3651–3655.
- Wyllie, A. H. (1980) *Nature (London)* **284**, 555–556.
- Cobrinik, D., Whyte, P., Peeper, D. S., Jacks, T. & Weinberg, R. A. (1993) *Genes Dev.* **7**, 2392–2404.
- Kastan, M. B., Zhan, Q., El-Deiry, W. S., Carrier, F., Jacks, T., Walsh, W. V., Plunkett, B. S., Vogelstein, B. & Fornace, A. J., Jr. (1992) *Cell* **71**, 587–597.
- Wu, X. & Levine, A. J. (1994) *Proc. Natl. Acad. Sci. USA* **91**, 3602–3606.
- Howes, K. A., Ransom, N., Papermaster, D. S., Lasudry, J. G. H., Albert, D. M. & Windle, J. J. (1994) *Genes Dev.* **8**, 1300–1310.
- Morgenbesser, S. D., Williams, B. O., Jacks, T. & DePinho, R. A. (1994) *Nature (London)* **371**, 72–74.
- Pan, H. & Griep, A. E. (1994) *Genes Dev.* **8**, 1285–1299.
- Lee, E. Y., Hu, N., Yuan, S., Cox, L. A., Bradley, A., Lee, W. H. & Herrup, K. (1994) *Genes Dev.* **8**, 2008–2021.
- Evan, G. I., Wyllie, A. H., Gilbert, C. S., Littlewood, T. D., Land, H., Brooks, M., Waters, C. M., Penn, L. Z. & Hancock, D. C. (1992) *Cell* **69**, 119–128.
- Lowe, S. W., Ruley, H. E., Jacks, T. & Housman, D. E. (1993) *Cell* **74**, 957–967.
- Hamel, P. A., Phillips, R. A., Muncaster, M. & Gallie, B. L. (1993) *FASEB J.* **7**, 846–854.